Selective Formation of Nanoholes with (100)-Face Walls by Photoetching of *n*-TiO_2 (Rutile) Electrodes, Accompanied by Increases in Water-Oxidation Photocurrent

Akira Tsujiko, Tetsuya Kisumi, Yoshifumi Magari, Kei Murakoshi, and Yoshihiro Nakato*

Department of Chemistry, Graduate School of Engineering Science, and Research Center for Photoenergetics of Organic Materials, Osaka University, Toyonaka, Osaka 560-8531, Japan

Received: September 15, 1999; In Final Form: November 19, 1999

Nanometer-sized rectangular holes or grooves in the ⟨001⟩ direction were formed when single-crystal rutile-type *n*-TiO_2 (001), (110), and (100) electrodes were illuminated in 0.05 M H_2SO_4 under anodic bias, accompanied by increases in water-oxidation photocurrents. Interestingly, only the (100) face was selectively exposed at the walls of the photoproduced holes and grooves, irrespective of crystal faces of electrode surfaces, though the (110) face for rutile TiO_2 is known to be the thermodynamically most stable, that is, to have the lowest surface Gibbs energy. On the other hand, no (100) face was exposed at the walls of rectangular holes produced by chemical etching with hot H_2SO_4 and hydrogen reduction at elevated temperatures, indicating that the selective exposition of the (100) face is characteristic of photoetching in H_2SO_4. A possible explanation is given by assuming that the selective exposition of the (100) face is due to a kinetics-controlled mechanism. It is tentatively suggested that the photoetching, which makes the surface structure changeable, may be much slower than the water photooxidation at the (100) surface, though not so much slower at other surfaces such as (110) and (001).

Introduction

It is well-known that n-type titanium dioxide (*n*-TiO_2) semiconductor electrodes are stable and can photooxidize water under anodic bias.[1] The elucidation of the molecular mechanism of the reaction will be helpful for searching for new active electrode materials for electrochemical oxygen evolution. The study of the mechanism of the reaction is also important from the point of view of improvement in the photocatalytic activity of TiO_2.

A number of studies have been made on the mechanism of the water-photooxidation reaction on single-crystal[2−17] and powdered[18] TiO_2 systems, using various methods including in situ photoluminescence (PL)[5,7,15−17] and electron spin resonance[18] measurements. However, reported mechanisms are still rather scattered and the detailed molecular mechanism has not been clarified yet. The main reason for such confusion may arise from a possibility that the reaction mechanism depends on detailed chemical structures of the electrode surface. Recently, Morris Hotsenpiller and co-workers reported[19,20] that sputter-deposited TiO_2 and polycrystalline TiO_2 films showed a prominent crystal face dependence in the efficiency of photocatalytic deposition of silver in an aqueous solution.

On the other hand, Harris and Wilson reported[21] that *n*-TiO_2 electrodes underwent photoinduced dissolution (photoetching) in aqueous H_2SO_4. Previously we reported[15] that a lot of rectangular long holes in the ⟨001⟩ direction were produced by illumination under anodic bias in aqueous H_2SO_4. Later, Sugiura et al. reported[22] the formation of similar rectangular holes and concluded that the nearly atomic flat (110) face was exposed at the walls of the photoformed holes. In the present paper, we report that not the (110) but the (100) face is selectively exposed at the walls,[23] though the (110) face is known to be the thermodynamically most stable. This result is of much interest, giving a rare and valuable example of selective exposition of surfaces other than the thermodynamically most stable surface by photoetching. This result is also of interest because it is likely to show crystal-face dependence of the photoetching and water-photooxidation rates.

Experimental Section

Single-crystal TiO_2 (rutile) wafers of 99.99% purity, 10 × 10 mm in area and 1.0 mm thick, having (001)-, (100)-, and (110)-cut and alkali-polished surfaces, were obtained from Earth Chemical Co. In our previous work,[15−17] the wafers were pretreated to get clean surfaces as follows: The wafers were polished with alumina powder of diameters 3.0, 1.0, 0.3, and 0.06 μm successively, etched in 66% H_2SO_4 containing 33% $(NH_4)_2SO_4$ at 240 °C for 30 min, washed, and annealed in air at 1300 °C for 4 h to remove defects by polishing. Then the wafers were slightly reduced by heating at about 700 °C in a stream of hydrogen to get n-type semiconductivity. Our recent experiments, however, revealed that the high-temperature annealing caused irreversible damage in TiO_2 crystals, giving a detrimental effect on the photoelectrochemical activity (cf. Figure 3). Thus, in the present work, the alkali-polished TiO_2 wafers[24] obtained from the company were simply washed with pure water and reduced in a stream of hydrogen at 700 °C for 30 min. The resistivity (ρ) of the reduced TiO_2 was measured by obtaining ohmic contacts with indium−gallium alloy on both faces of the wafer. Specimens of 0.2 to 1.0 Ω cm were used for experiments. The indium−gallium alloy was then removed by immersing the wafer in a hydrogen chloride solution, and the alloy was painted again on one face of the wafer for electrode preparation.

Single-crystal TiO_2 (rutile) wafers doped with 0.035 and 0.050 wt % niobium oxide were also obtained from Earth Chemical

* Author for correspondence. Fax +81−6−6850−6236; e-mail nakato@chem.es.osaka-u.ac.jp.

10.1021/jp993285e CCC: $19.00
Published on Web 04/29/2000

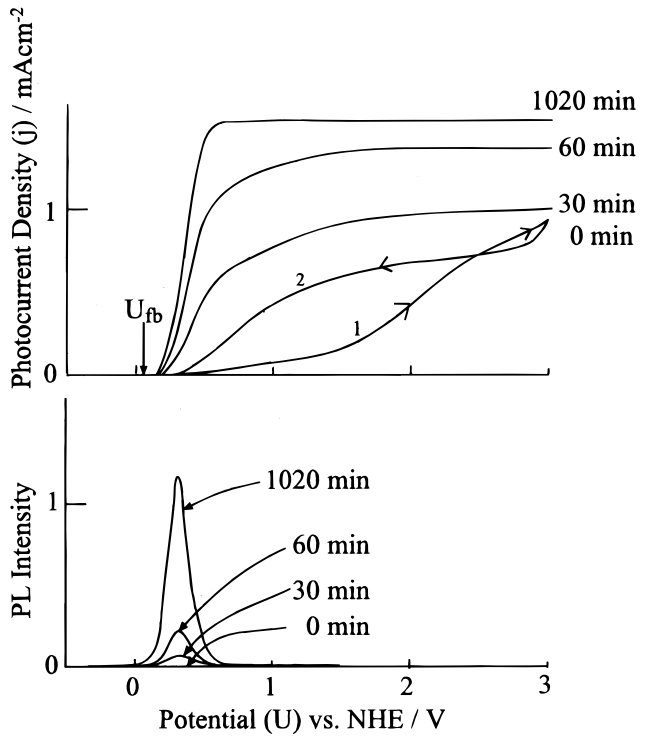

Figure 1. The *j-U* and PL intensity−*U* curves in 0.05 M H_2SO_4 (pH 1.2) for an *n*-TiO_2(001) electrode freshly prepared by H_2 reduction at 700 °C. 1: The first (positive) potential scan, and 2: the succeeding negative potential scan. The times indicated in the figure refer to the time that elapsed from the start of electrode illumination. The U_{fb} is the reported flat-band potential for rutile-type *n*-TiO_2 (+0.05 V versus NHE at pH 0).[25,26]

Co. They were 10 × 10 mm in area and 1.0 mm thick and had (001)-, (100)-, and (110)-cut and alkali-polished surfaces. The Nb-doped TiO_2 is an n-type semiconductor without any pretreatment, because doped Nb^{3+} acts as an electron donor.

Photocurrent density (*j*) versus potential (*U*) curves were measured with a commercial potentiostat and a potential programmer, using a Pt plate (2 × 3 cm^2) as the counterelectrode and an Ag/AgCl/sat. KCl electrode as the reference electrode. Illumination was performed by a 365-nm band from a 500-W high-pressure mercury lamp, obtained by use of band-pass filters. Photoluminescence PL spectra were measured with a Jobin−Yvon H20IR monochromator and a Hamamatsu Photonics R316 or R712 photomultiplier cooled at −20 °C. PL intensity versus *U* curves were measured simultaneously with the *j-U* curve measurements. The structure of electrode surface was inspected with a high-resolution scanning electron microscope (Hitachi, S-5000) and an atomic force microscope (Digital Instruments, Nanoscope IIIa).

Electrolyte solutions were prepared by use of reagent grade chemicals and water purified from deionized water with a Milli-Q water purification system. The electrolyte solution was stirred magnetically and kept at 20 ± 0.3 °C during measurements. The concentration unit, mol/dm^3, is abbreviated as M in the present paper.

Results

Figure 1 shows *j* versus *U* curves in 0.05 M H_2SO_4 (pH 1.2), together with PL intensity versus *U* curves, for an *n*-TiO_2(001) electrode freshly prepared by a simple pretreatment of water-washing and H_2 reduction at 700 °C (see the *Experimental Section*). [We hereafter designate *n*-TiO_2 electrodes having the (001)-cut surface as *n*-TiO_2(001), in which the (001) does not mean the atomically flat (001) surface. The same holds for *n*-TiO_2(110) and (100) electrodes described later.] The photocurrent density is calculated by using the apparent (not true) area of the electrode surface. The reported flat-band potential (U_{fb}) for rutile-type *n*-TiO_2 [+0.05 V versus normal hydrogen electrode (NHE) at pH 0][25,26] is indicated for reference with a pH correction of 0.059 V/pH. The first positive (curve 1) and negative (curve 2) potential scans for a freshly prepared electrode showed only low photocurrents and no PL. However, successive repeated (continuous) potential scans between 0.0 and 3.0 V at a rate of 50 mV/s under illumination in 0.05 M H_2SO_4 improved the *j-U* curve very much, together with an appearance of the PL band peaking at 840 nm near the onset potential of the photocurrent, U_{on}. The same results were obtained at other scan rates and when the illumination and potential scans were carried out intermittently. Once activated, electrodes kept the high activity and strong PL in aqueous solutions of any pH unless they were polished.

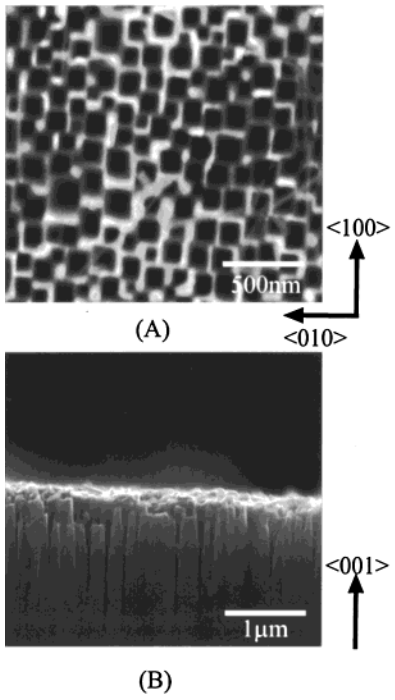

Figure 2. SEMs for the surface (A) and cross-section (B) of an activated *n*-TiO_2(001) electrode that gave the most improved *j-U* curve in Figure 1.

Figure 2 shows scanning electron micrographs (SEMs) for the surface and cross-section of an *n*-TiO_2(001) electrode that gives the most improved *j-U* curve in Figure 1. A large number of rectangular holes, 50−200 nm wide and about 1 μm long, are produced with a fairly regular arrangement. From the crystal-cut faces indicated in Figure 2, we can see that the rectangular holes extend in the ⟨001⟩ direction and that the (100) face or equivalents are exposed selectively at the walls. These results indicate clearly that the electrode activation in Figure 1 is caused by photoetching of the *n*-TiO_2 electrode, which occurs in 0.05 M H_2SO_4 slightly and competitively with the photooxidation reaction of water.

Detailed experiments showed that the improvement in the *j-U* curve in Figure 1 occurred by two steps as explained below: The surfaces of alkali-polished TiO_2(001) obtained from the company were smooth within a roughness of 1 to 2 nm as inspected by atomic force microscopy. The hydrogen reduction at 700 °C for 30 min produced holes (or pits) with an inverse-pyramid shape here and there as explained later (cf. Figure 8),

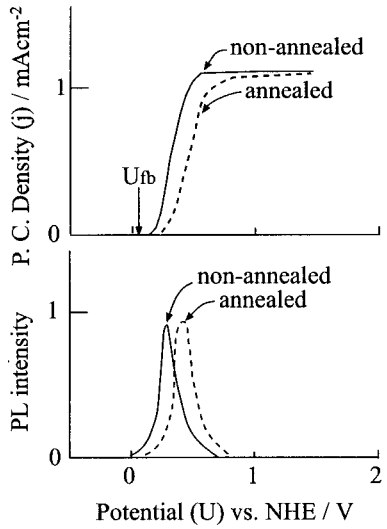

Figure 3. Most-improved *j*-*U* curve for a high-temperature annealed *n*-TiO_2(001) electrode (solid curve) as compared with that for a nonannealed electrode (broken curve), together with a change in the PL intensity−*U* curve.

but most other parts of the surface remained smooth. After the positive and negative potential scans (curves 1 and 2) in Figure 1, the surface still remained smooth with no formation of the rectangular holes, though the shape of the *j*-*U* curve was considerably improved. This suggests that the rectangular holes grow after such initial improvement in the *j*-*U* curve. In fact, a lot of tiny rectangular holes (pits) started to appear at the smooth surface after the initial positive and negative potential scans (curves 1 and 2 in Figure 1). Thus, the initial improvement in the *j*-*U* curve (curves 1 and 2 in Figure 1) can be attributed to removal of a certain thin inactive layer (such as an amorphous TiO_2 layer) formed on the *n*-TiO_2 surface during the H_2 reduction at 700 °C (and successive reoxidation in air). The inverse-pyramid holes produced by the H_2 reduction disappear in Figure 2, owing to progress of photoetching at the TiO_2 surface under prolonged illumination.

The formation of a thin inactive layer on the *n*-TiO_2 surface during the H_2 reduction at 700 °C (and successive reoxidation in air) is supported by the following fact. In previous papers[15−17] we reported similar electrode activation and nanohole formation for freshly prepared *n*-TiO_2(001) electrodes that were prepared by a pretreatment including high-temperature annealing at 1300 °C (see *Experimental Section*), contrary to the present work. An important difference between the previous and present results is that the most-improved *j*-*U* curve for the high-temperature annealed electrodes is shifted toward the positive by about 0.10 V relative to that for the nonannealed electrodes, as is shown in Figure 3. This indicates that the high-temperature annealing caused considerable damages in TiO_2 crystals, giving a detrimental effect on the *j*-*U* curve. It is expected that the H_2 reduction at a high temperature of 700 °C caused similar damages near the TiO_2 surface, though to a lesser extent than at 1300 °C.

Figure 4 shows the *j*-*U* and PL intensity−*U* curves for an *n*-TiO_2(110) electrode, and Figure 5 shows SEMs for the most activated *n*-TiO_2(110) electrode, both illustrated in the same way as Figures 1 and 2, respectively. The *j*-*U* curve was improved by two steps, with the initial improvement (curves 1 and 2 in Figure 4) followed by the succeeding improvement (curves denoted by 50 and 180 min), similar to the case of the *n*-TiO_2-(001) electrodes. The PL near U_{on} became strong in parallel with the succeeding improvement, also similar to the case of

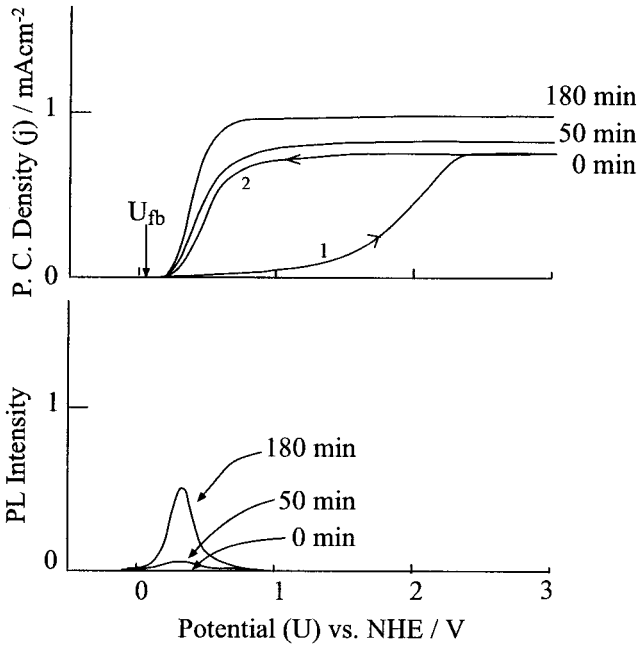

Figure 4. *j*-*U* and PL intensity−*U* curves for a freshly prepared *n*-TiO_2-(110) electrode, illustrated in the same way as Figure 1.

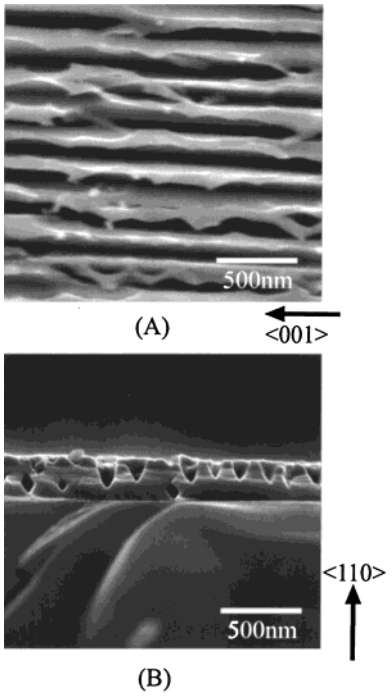

Figure 5. SEMs for an *n*-TiO_2(110) electrode activated by illumination in 0.05 M H_2SO_4 under potential scans for 180 min, illustrated in the same way as Figure 2.

n-TiO_2(001). However, for *n*-TiO_2(110), rectangular long grooves were produced at the electrode surface in the ⟨001⟩ direction. The cross-sectional SEM shows that the walls of the grooves are inclined at about 45° against the electrode surface, indicating that the (100) face or equivalents are exposed at the walls of the grooves.

Figures 6 and 7 show the results for an *n*-TiO_2(100) electrode, illustrated in the same way as Figures 1 and 2. The results are quite similar to those for the *n*-TiO_2(110) electrode in Figures 4 and 5, except that the walls of the photoproduced grooves are in parallel with or perpendicular to the electrode surface. This also shows that the (100)-face or equivalents are exposed

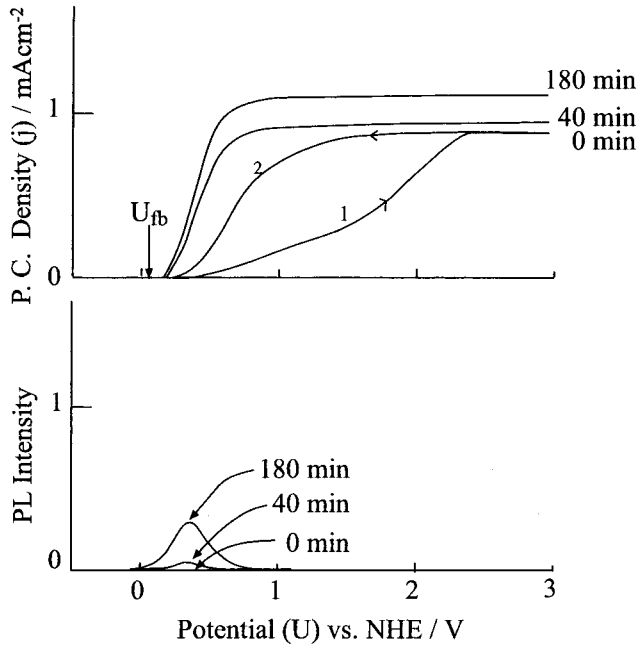

Figure 6. The *j*-*U* and PL intensity−*U* curves for a freshly prepared *n*-TiO_2(100) electrode, illustrated in the same way as Figure 1.

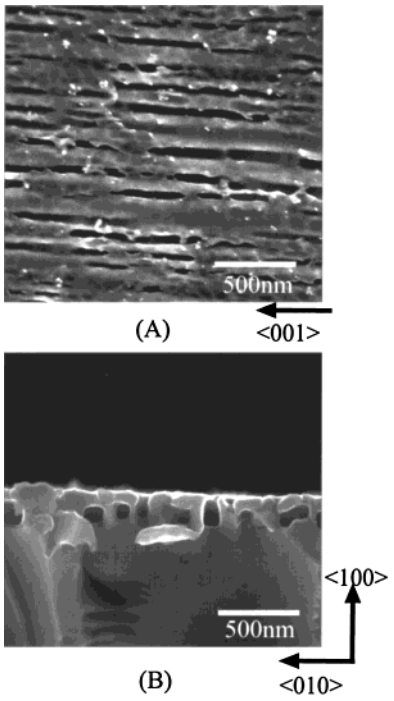

Figure 7. SEMs for an *n*-TiO_2(100) electrode activated by illumination in 0.05 M H_2SO_4 under potential scans for 180 min, illustrated in the same way as Figure 2.

at the walls. It may be important to mention here that the *j*-*U* curves for the most activated *n*-TiO_2(001), (110), and (100) electrodes nearly agreed with each other.

Experiments were also done under illumination at constant potentials. The same results as described thus far were obtained when the electrode potential was kept at potentials where the illumination intensity-limited photocurrents were observed, say, +2.2 V versus NHE. Namely, rectangular holes for the (001) electrodes and rectangular grooves for the (100) electrodes were produced, with only the (100) face or equivalents being exposed at the walls, together with the increases in the water-oxidation photocurrents. The electricity passing across the electrode

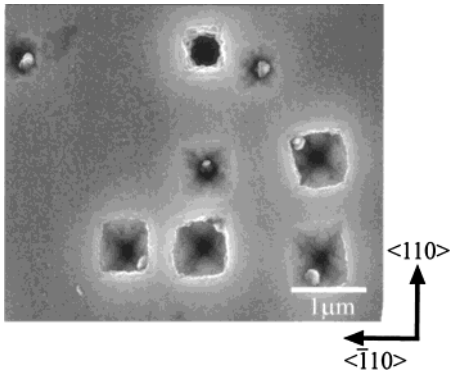

Figure 8. SEM for the surface of TiO_2(001) after a hydrogen-reduction treatment at 700 °C for 30 min.

surface ranged from 30 to 50 C/cm^2 for the apparent area of the electrode surface. The holes or grooves grew simply with the increasing electricity. However, the illumination at potentials where the illumination intensity-limited photocurrent was not reached yet, say, +0.3 V, produced no holes even though the same electricity as above passed.

Experiments were also done using 0.035 wt % Nb-doped *n*-TiO_2(001), (110), and (100) electrodes ($\rho = 8\sim9\ \Omega$ cm). The illumination was performed either under cyclic potential scans between 0 and 3 V or at a constant potential of 2.2 V versus NHE. In both cases, the same results as the case of H_2-reduced *n*-TiO_2 electrodes were obtained, that is, rectangular holes in the ⟨001⟩ direction were produced, with only the (100) face or equivalents being exposed at the walls, together with the increases in the water-oxidation photocurrent. A difference is that the "initial improvement" such as shown in curves 1 and 2 in Figures 1, 4, and 6 was observed only for the H_2-reduced *n*-TiO_2, supporting the aforementioned explanation that the initial improvement arises from an effect of the H_2 reduction procedure at 700 °C. When 0.050 wt % Nb-doped *n*-TiO_2(001) was used, the number of rectangular holes per unit area increased a little, accompanied by a slight decrease in their size.

To investigate why the (100) face or equivalents are selectively exposed at the walls of the photoproduced holes and grooves, we did some experiments. First we found that the hydrogen reduction of TiO_2(001) at 700 °C also produced rectangular holes (or pits) with an inverse-pyramid shape (Figure 8). However, the edges of the holes at the surface were nearly parallel with the ⟨110⟩ direction or equivalents and no (100) face was exposed at the walls of the holes.

Next, we examined the effect of chemical etching with H_2SO_4 because the aforementioned photoetching occurred only in aqueous H_2SO_4. Figure 9 shows an SEM of an *n*-TiO_2(001) surface after being chemically etched with 66% H_2SO_4 containing 33% $(NH_4)_2SO_4$ at 240 °C for 30 min. Holes (etch pits) with an inverse-pyramid shape were produced, but no (100) face was exposed, similarly to the case of the hydrogen reduction at 700 °C. The formation of similar holes by chemical etching with H_2SO_4 was reported by Miki and Yanagi.[27]

The production of the rectangular holes with different orientations between the photoetching in H_2SO_4 and the hydrogen reduction at 700 °C was clearly seen by an experiment shown in Figure 10. A TiO_2(001) wafer was first reduced under hydrogen at 700 °C, which produced holes (pits) with an inverse-pyramid shape such as shown in Figure 8. Then a half of the H_2-reduced *n*-TiO_2 wafer (electrode) was illuminated in 0.05 M H_2SO_4 under anodic bias. In the nonilluminated part, no photoetching proceeded and thus the inverse-pyramid holes produced upon the H_2 reduction remained. On the other hand,

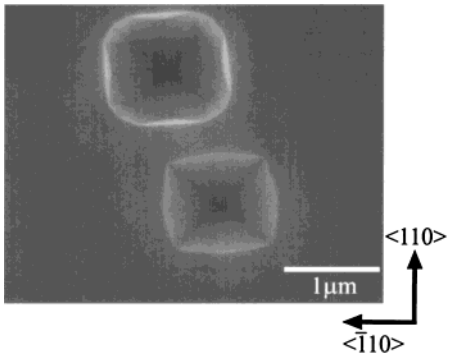

Figure 9. SEM for the surface of *n*-TiO_2(001) after being chemically etched with 66% H_2SO_4 containing 33% $(NH_4)_2SO_4$ at 240 °C for 30 min.

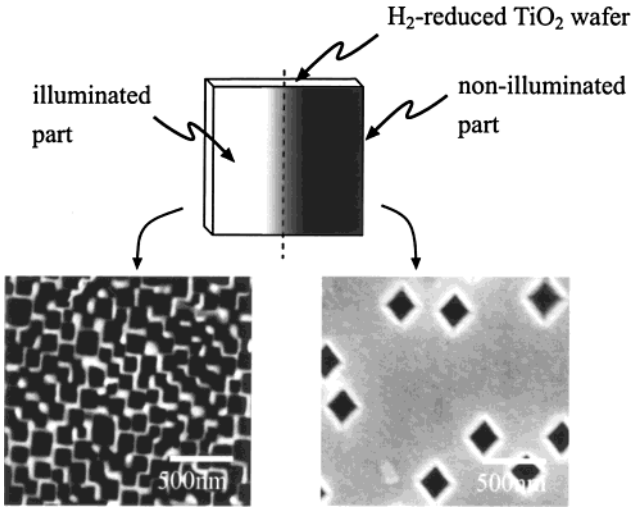

Figure 10. SEMs of a hydrogen-reduced *n*-TiO_2(001) surface, half of which was later illuminated and photoetched in H_2SO_4.

in the illuminated part, the photoetching proceeded and a lot of deep rectangular holes were produced, similarly to the case of Figure 2. It is to be noted that the orientation of the edges of the rectangular holes at the surface is different by 45° from each other, confirming that holes with different orientations were produced by these procedures.

Discussion

The experimental results described in the preceding section can be summarized as follows. (a) Nanosized rectangular long holes or grooves, extending in the ⟨001⟩ direction and having selectively the (100) face at the walls, were produced by illumination of *n*-TiO_2 (rutile) in H_2SO_4 under anodic bias, irrespective of the crystal faces of the electrode surfaces (Figures 2, 5, and 7). The same results were obtained for H_2-reduced and Nb-doped *n*-TiO_2 electrodes. (b) The *j-U* curve was improved and the PL band peaking at 840 nm appeared (Figures 1, 4, and 6), in parallel with the formation and growth of the rectangular holes or grooves, for both the H_2-reduced and Nb-doped *n*-TiO_2 electrodes. For H_2-reduced *n*-TiO_2, however, the improvement in the *j-U* curve showed the additional initial improvement (curves 1 and 2 in Figuress 1, 4, and 6) independent of the formation of the rectangular holes and the appearance of the PL. (c) Chemical etching with hot H_2SO_4 as well as hydrogen reduction at 700 °C also produced rectangular holes having an inverse-pyramid shape, but no (100) face was exposed at the walls (Figures 8 and 9). (d) The annealing at

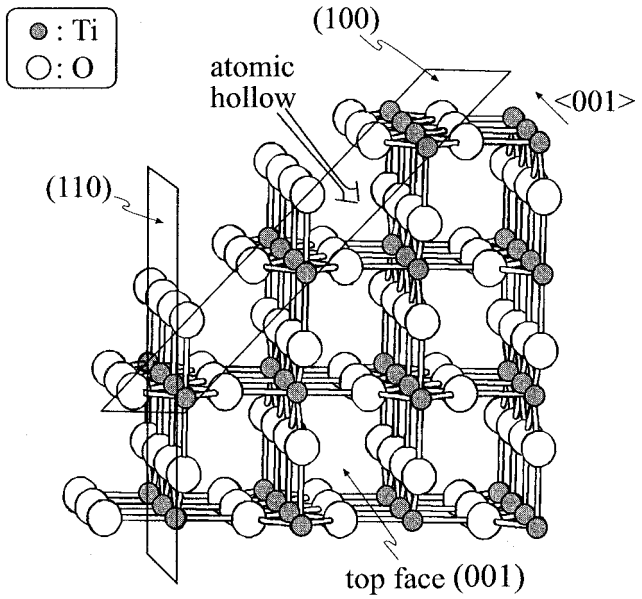

Figure 11. Model of crystal structure for TiO_2 (rutile), together with possible atomic arrangements at the (001), (110), and (100) faces.

high temperatures such as 1300 °C caused severe damages in TiO_2 crystals, giving a detrimental effect on the *j-U* curve (Figure 3).

It is reported[28−30] that the annealing at temperatures higher than about 500 °C causes more or less reconstruction at the surface by surface spectroscopy and scanning tunneling microscopy. The positive shift in the *j-U* curve for *n*-TiO_2 electrodes prepared by a pretreatment including the high-temperature annealing at 1300 °C relative to that for nonannealed electrodes (Figure 3) can be attributed to such reconstruction (or deformation) for the former electrodes. The reconstruction for such high-temperature annealing cannot be removed completely even by photoetching under prolonged illumination, indicating that the deformation proceeds considerably deep in the bulk of crystals. The aforementioned initial improvement for the H_2-reduced *n*-TiO_2 electrodes can be attributed to removal of a thin inactive surface layer produced by such surface reconstruction during the H_2 reduction at 700 °C.

As mentioned in the preceding section, it is certain that the formation of the rectangular holes and grooves at the *n*-TiO_2 surfaces is caused by photoetching in aqueous H_2SO_4, which occurs slightly and competitively with the photooxidation reaction of water. Sugiura et al. reported[22] that the photoetching for sintered polycrystalline *n*-TiO_2 (rutile) electrodes proceeded at a ratio of a few percentages of the whole photoanodic reactions. The formation of long holes or grooves in the ⟨001⟩ direction indicates that the photoetching proceeds fast in this direction. This can be understood if we take into account that the photoetching proceeds fast along crystalline channels of rutile-type TiO_2 present in the ⟨001⟩ direction (see a crystal-structure model in Figure 11). The increase in the number of rectangular holes with the increasing density of Nb for Nb-doped *n*-TiO_2, mentioned in the preceding section, may suggest that the hole formation is initiated by certain defects introduced by Nb doping.

The present work has revealed clearly that only the (100) face or equivalents are selectively exposed at the walls of photoproduced rectangular holes and grooves. It is reported that the thermodynamically most stable surface (i.e. the surface having the lowest surface Gibbs energy) is apt to be exposed after etching.[31,32] For rutile TiO_2, experimental[28−30] and theoreti-

cal[33] studies showed that the (110) face is the thermodynamically most stable. Thus, the above result is of much interest, giving a rare and valuable example of the selective exposition of surfaces other than the thermodynamically most stable surface by photoetching.

Little is clear at present about the mechanism of the selective exposition of the (100) face. It is evident from the above argument that this result cannot be explained by a usual thermodynamics-controlled mechanism, in which the thermodynamically most stable surface is left after etching. An alternative mechanism is to assume that it is due to a kinetics-controlled mechanism in which the kinetically most stable surface is left after etching. No exposition of the (100) face by chemical H_2SO_4 etching (Figure 9) indicates that the exposition of the (100) face by photoetching in H_2SO_4 is not due to a specific action of H_2SO_4. Also, that the same results were obtained for H_2-reduced and Nb-doped *n*-TiO_2, as mentioned in the preceding section, will exclude a possibility of an unknown specific role of hydrogen atoms that may be incorporated upon the H_2 reduction pretreatment.

Thus, it might tentatively be assumed that, at the (100) face, the photoetching that leads to a change in the surface structure is much slower than the water photooxidation, though not so much slower at other surfaces such as (001) and (110). If this is the case, photogenerated holes coming to the (100) surface are mostly consumed for the water oxidation and thus the (100) surface is kept kinetically stable. On the other hand, photogenerated holes coming to other surfaces such as (001) and (110) cause the photoetching to some extent, competitively with the water oxidation. Thus the surfaces such as (001) and (110) will change to other faces gradually. Such processes finally lead to the exposition of the (100) face after prolonged illumination. Further details are now under investigation.

Another notable point is that the *j-U* curve is improved and the PL band at 840 nm appears both in parallel with the formation of the rectangular holes and grooves. The increases in the illumination intensity-limited photocurrents in 0.5 to 3.0 V versus NHE in Figures 1, 4, and 6 can be attributed mainly to decreases in light reflection at the electrode surface by formation of the holes or grooves. The increases in photocurrents in their rising parts in 0.1 to 0.5 V occur at a higher ratio than those in the illumination intensity-limited photocurrents, showing the real activation of the electrodes. This fact was emphasized in our previous paper (see Figure 2 of ref 15). The photocurrents in the rising parts will be determined mainly by a competition of the water-oxidation reaction and surface carrier recombination via oxidative reaction intermediates. Therefore their increases may be attributed to decreases in the surface carrier recombination either by exposition of the atomically well-defined (100) face or by increases in the true electrode area through the formation of the holes or grooves.

It is to be noted also that the intensity of the PL band increases with the exposition of the (100) face. In previous papers[16,17] we reported that Ti−OH in a bulk defect (such as atomic gaps) near the surface was oxidized (by valence-band holes) more easily than Ti−OH at the surface. We also reported that the PL band could be assigned to an electronic transition from conduction-band electrons to a vacant (O 2p) level of an oxidative surface intermediate (probably Ti−O· radicals) in the bulk defect. The (100) surface has a kind of "atomic hollows" or "atomic grooves", as indicated in Figure 11. Thus, the above result may suggest that the atomic hollows or grooves in the (100) face act as a kind of the bulk defect (atomic gaps), leading to a higher rate of the water photooxidation at this face.

It may look apparently contradictory that the increases in photocurrents in their rising parts in 0.1 to 0.5 V are accompanied by the appearance of the PL band (Figures 1, 4, and 6), because the latter shows an increase in the surface recombination. It is to be noted here that, even for the most improved *j-U* curve, the photocurrent onset (U_{on}) is shifted from the flat-band potential (U_{fb}) toward the positive by about 0.15 V, suggesting that a certain kind of surface recombination is still present. This surface recombination can give rise to the PL. This explanation is supported by the reported fact[5,7] that the addition of a reductant such as hydroquinone to the solution causes a shift of U_{on} to U_{fb}, accompanied by the disappearance of PL. Thus, the above-mentioned increases in photocurrents in their rising parts can be attributed to removal of other-type surface recombination via surface defects introduced by polishing or surface reconstruction by the exposition of the atomically well-defined (100) face.

In conclusion, the present work has revealed that the photoetching of *n*-TiO_2 (rutile) in aqueous H_2SO_4 produces nanometer-sized rectangular holes, extending in the ⟨001⟩ direction and having selectively the (100) face at the walls, with a fairly regular arrangement. It is important to note that the (100) face is exposed only by photoetching in H_2SO_4 and is not the thermodynamically most stable surface. These results are of much interest, giving a rare example of selective exposition of nonstable surfaces and suggesting a possibility of crystal-face dependence of the rates of photoetching or water-photooxidation reactions. Further studies will lead not only to clarification of the photoetching and water-photooxidation mechanisms but also to a new technique in nanostructuring of semiconductor surfaces.

Acknowledgment. This work was partly supported by a grant-in-aid for scientific research on priority area of electrochemistry of ordered interfaces (no. 09237105) from the Ministry of Education, Science, Sports, and Culture, Japan.

References and Notes

(1) Fujishima, A.; Honda, K. *Nature* (*Londgon*) **1972**, *238*, 37.
(2) Augustynski, J. *Struct. Bonding* (*Berlin*) **1988**, *69*, 1.
(3) Wilson, R. H. *J. Electrochem. Soc.* **1980**, *127*, 228.
(4) Salvador, P. *J. Electrochem. Soc.* **1981**, *128*, 1895.
(5) Nakato, Y.; Tumura, A.; Tsubomura, H. *J. Phys. Chem.* **1983**, *87*, 2402.
(6) Salvador, P.; Gutierrez, C. *J. Phys. Chem.* **1984**, *88*, 3696.
(7) Nakato, Y.; Ogawa, H.; Morita, K.; Tsubomura, H. *J. Phys. Chem.* **1986**, *90*, 6210.
(8) Kasinski, J. J.; Gomez-Jahn, L. A.; Faran, K. J.; Gracewski, S. M.; Dwayne Miller, R. J. *J. Chem. Phys.* **1989**, *90*, 1253.
(9) Taffala, D.; Salvador, P.; Benito, R. M. *J. Electrochem. Soc.* **1990**, *137*, 1810.
(10) Kiwiet, N.; Fox, M. A. *J. Electrochem. Soc.* **1990**, *137*, 561.
(11) Garcia Gonzalez, M. L,; Salvador, P. *J. Electroanal. Chem.* **1992**, *325*, 369.
(12) Nogami, G.; Sei, H.; Aoki, A.; Ohkubo, S. *J. Electrochem. Soc.* **1994**, *141*, 3410.
(13) Salama, S. B.; Natarajan, C.; Nogami, G.; Kennedy, J. H. *J. Electrochem. Soc.* **1995**, *142*, 806.
(14) Shaw, K.; Christensen, P.; Hamnett, A. *Electrochim. Acta* **1996**, *41*, 719.
(15) Nakato, Y.; Akanuma, H.; Shimizu, J.-I.; Magari, Y. *J. Electroanal. Chem.* **1995**, *396*, 35.
(16) Magari, Y.; Ochi, H.; Yae, S.; Nakato, Y. *Solid/Liquid Electrochemical Interfaces*; ACS Symposium Series 656; American Chemical Society: Washington, DC, 1996; p. 297.
(17) Nakato, Y.; Akanuma, H.; Magari, Y.; Yae, S.; Shimizu, J.-I.; Mori, H. *J. Phys. Chem. B* **1997**, *101*, 4934.
(18) Nakaoka, Y.; Nosaka, Y. *J. Photochem. Photobiol. A* **1997**, *110*, 299, and papers cited therein.
(19) Morris Hotsenpiller, P. A.; Bolt, J. D.; Farneth, W. E.; Lowekamp, J. B.; Rohrer, G. S. *J. Phys. Chem. B* **1998**, *102*, 3216.
(20) Lowekamp, J. B.; Rohrer, G. S.; Morris Hotsenpiller, P. A.; Bolt, J. D.; Farneth, W. E. *J. Phys. Chem. B* **1998**, *102*, 7323.

(21) Harris, L. A.; Wilson, R. H. *J. Electrochem. Soc*. **1976**, *123*, 1010.
(22) Sugiura, T.; Yoshida, T.; Minoura, H. *Electrochem. Solid-State Lett*. **1998**, *1*, 175.
(23) Recently Sugiura et al. changed their conclusion from the exposition of the (110) face to the (100) face (a private communication).
(24) The details of the alkali polishing adopted in the company are unknown, being kept secret.
(25) Butler, M.; Ginley, D. S. *J. Electrochem. Soc*. **1979**, *125*, 228.
(26) Tomkiewicz, M. J. *J. Electrochem. Soc.* **1979**, *126*, 1505.
(27) Miki, T.; Yanagi, H. *Langmuir* **1998**, *14*, 3405.
(28) Tait, R. H.; Kasowski, R. V. *Phys. Rev. B* **1979**, *20*, 5178.
(29) Poirier, G. E.; Hance, B. K.; White, J. M. *J. Vac. Sci. Technol., B* **1992**, *10*, 6.
(30) Linsebigler, A. L.; Lu, G. Q.; Yates, J. T., Jr. *Chem. Rev*. **1995**, *95*, 735, and papers cited therein.
(31) Jakob, P.; Chabal, Y. J. *J. Chem. Phys*. **1991**, *95*, 2897.
(32) Allongue, P.; Costa-Kieling, V.; Gerischer, H. *J. Electrochem. Soc.* **1993**, *140*, 1009 and 1018.
(33) Kasowski, R. V.; Tait, R. H. *Phys. Rev. B* **1979**, *20*, 5168.